AMERICAN ACADEMY™ OF OPHTHALMOLOGY

Projection-Resolved Optical Coherence Tomography Angiography of Macular Retinal Circulation in Glaucoma

Hana L. Takusagawa, MD, Liang Liu, MD,* Kelly N. Ma, MD, MPH, Yali Jia, PhD, Simon S. Gao, PhD, Miao Zhang, PhD, Beth Edmunds, MD, PhD, Mansi Parikh, MD, Shandiz Tehrani, MD, PhD, John C. Morrison, MD, David Huang, MD, PhD*

Purpose: To detect macular perfusion defects in glaucoma using projection-resolved optical coherence tomography (OCT) angiography.

Design: Prospective observation study.

Participants: A total of 30 perimetric glaucoma and 30 age-matched normal participants were included.

Methods: One eye of each participant was imaged using 6×6−mm macular OCT angiography (OCTA) scan pattern by 70-kHz 840-nm spectral-domain OCT. Flow signal was calculated by the split-spectrum amplitude-decorrelation angiography algorithm. A projection-resolved OCTA (PR-OCTA) algorithm was used to remove flow projection artifacts. Four en face OCTA slabs were analyzed: the superficial vascular complex (SVC), intermediate capillary plexus (ICP), deep capillary plexus (DCP), and all-plexus retina (SVC + ICP + DCP). The vessel density (VD), defined as the percentage area occupied by flow pixels, was calculated from en face OCTA. A novel algorithm was used to adjust the vessel density to compensate for local variations in OCT signal strength.

Main Outcome Measures: Macular retinal VD, ganglion cell complex (GCC) thickness, and visual field (VF) sensitivity.

Results: Focal capillary dropout could be visualized in the SVC, but not the ICP and DVP, in glaucomatous eyes. In the glaucoma group, the SVC and all-plexus retinal VD (mean ± standard deviation: 47.2%±7.1% and 73.5%±6.6%) were lower than in the normal group (60.5%±4.0% and 83.2%±4.2%, both $P < 0.001$, *t* test). The ICP and DCP VD were not significantly lower in the glaucoma group. Among the overall macular VD parameters, the SVC VD had the best diagnostic accuracy as measured by the area under the receiver operating characteristic curve (AROC). The accuracy was even better when the worse hemisphere (inferior or superior) was used, achieving an AROC of 0.983 and a sensitivity of 96.7% at a specificity of 95%. Among the glaucoma participants, the hemispheric SVC VD values were highly correlated with the corresponding GCC thickness and VF sensitivity ($P < 0.003$). The reflectance compensation step in VD calculation significantly improved repeatability, normal population variation, and correlation with VF and GCC thickness.

Conclusions: On the basis of PR-OCTA, glaucoma preferentially affects perfusion in the SVC in the macula more than the deeper plexuses. Reflectance-compensated SVC VD measurement by PR-OCTA detected glaucoma with high accuracy and could be useful in the clinical evaluation of glaucoma. *Ophthalmology 2017;124:1589-1599 © 2017 by the American Academy of Ophthalmology*

Supplemental material available at www.aaojournal.org.

See Editorial on page 1577.

Glaucoma is the second leading cause of blindness worldwide, affecting more than 60 million people and predicted to affect 79.6 million by 2020.[1−3] Early diagnosis and close monitoring of glaucoma are important given glaucoma's insidious onset with irreversible nerve damage associated with vision loss. Although studies of glaucoma traditionally have focused on the optic nerve and peripapillary retina, there are multiple reasons to evaluate the macula in glaucoma diagnosis and monitoring.

Histologic studies have shown that glaucoma results in loss of retinal ganglion cells (RGCs) and more than 30% of the ganglion cells in the eye reside in the macula.[4,5] Many recent optical coherence tomography (OCT) studies have shown that macular thinning is associated with glaucoma and that the thinning preferentially affects the ganglion cell complex (GCC), the innermost layers of the retina, which include the retinal nerve fiber layer (NFL), ganglion cell layer (GCL), and inner plexiform layer (IPL).[6−8] Diagnostic accuracy for glaucoma can be improved when macular OCT measurements focus particularly on the GCC.[6,9,10] Given that a preponderance of RGCs reside in the macula, studies have suggested that early glaucomatous damage involves the macula.[11] Recent studies have shown that early visual field (VF) loss often occurs in the central 10 degrees of

http://dx.doi.org/10.1016/j.ophtha.2017.06.002
ISSN 0161-6420/17

vision, an area represented by the macula.[12] Focal loss of the GCC on OCT appears to be an excellent predictor of progression from preperimetric to perimetric glaucoma.[13]

Optical coherence tomography angiography (OCTA) with the split-spectrum amplitude-decorrelation angiography algorithm has provided a quick and reproducible way to qualitatively and quantitatively show areas of decreased or altered perfusion in the eye.[14–19] By using OCTA, Jia et al[14] demonstrated significantly decreased perfusion at the optic nerve head in glaucoma and Liu et al[15] similarly showed decreased perfusion in the peripapillary retina. Previous OCTA investigations in glaucoma macular circulation used 3×3−mm scan, which though able to demonstrate glaucoma damage in some patients but had poor diagnostic accuracy overall.[20–22] Thus, we investigate larger OCTA scans at 6×6−mm square size that covers areas likely to be affected by glaucoma.[11] More recently, we developed a "projection-resolved" algorithm that effectively suppresses projection artifacts on both en face and cross-sectional angiograms and enhances depth resolution of vascular networks.[23,24] By using projection-resolved OCTA (PR-OCTA), we are now able to visualize the distinct vascular patterns in the 4 retinal plexuses. This study aims to compare the macular circulation in normal participants and glaucomatous participants in different retinal plexuses and to detect and characterize macular circulation defects in glaucoma using PR-OCTA.

Methods

Study Population

This prospective observation study was performed from September 16, 2014, to February 20, 2016, at the Casey Eye Institute, Oregon Health & Science University (OHSU). The research protocols were approved by the Institutional Review Board at OHSU, carried out in accordance with the tenets of the Declaration of Helsinki. Written informed consent was obtained from each participant.

All participants were part of the Functional and Structural Optical Coherence Tomography for Glaucoma study. The inclusion criteria for the perimetric glaucoma group were (1) an optic disc rim defect (thinning or notching) or NFL defect visible on slit-lamp biomicroscopy; and (2) a consistent glaucomatous pattern, on both qualifying Humphrey Swedish Interactive Thresholding Algorithm 24-2 VFs, meeting at least 1 of the following criteria: pattern standard deviation outside normal limits ($P < 0.05$) or glaucoma hemifield test outside normal limits.

For the normal group, the inclusion criteria were (1) no evidence of retinal pathology or glaucoma; (2) a normal Humphrey 24-2 VF; (3) intraocular pressure (IOP) <21 mmHg; (4) central corneal pachymetry >500 μm; (5) no chronic ocular or systemic corticosteroid use; (6) an open angle on gonioscopy; (7) a normal-appearing optic nerve head and NFL; and (8) symmetric optic nerve head between left and right eyes.

The exclusion criteria for both groups were (1) best-corrected visual acuity <20/40; (2) age <30 or >80 years; (3) refractive error of >+3.00 diopters or <−7.00 diopters; (4) previous intraocular surgery except for an uncomplicated cataract extraction with posterior chamber intraocular lens implantation; (5) any diseases that may cause VF loss or optic disc abnormalities; or (6) inability to perform reliably on automated VF testing. One eye from each participant was scanned and analyzed.

Visual Field Testing

The VF tests were performed with the Humphrey Field Analyzer II (Carl Zeiss, Inc, Oberkochen, Germany) set for the 24-2 threshold test, size III white stimulus, using the Swedish Interactive Thresholding Algorithm.

Optical Coherence Tomography

A 70-kHz, 840-nm wavelength spectral-domain OCT system (Avanti RTVue-XR, Optovue Inc, Fremont, CA) was used. The AngioVue version 2014.1.0.2 software was used to acquire OCTA scans.

Image Acquisition and Processing

The macular region was scanned using a 6×6−mm volumetric angiography scan centered on fixation. Each volume was composed of 304 line-scan locations at which 2 consecutive B-scans were obtained. Each B-scan contains 304 A-scans. The AngioVue software uses the split-spectrum amplitude-decorrelation angiography algorithm, which compares the consecutive B-scans at the same location to detect flow using motion contrast.[25] Each scan set comprises 2 volumetric scans: 1 vertical-priority raster and 1 horizontal-priority raster. The AngioVue software uses an orthogonal registration algorithm to register the 2 raster volumes to produce a merged 3-dimensional OCTA.[26] Two sets of scans were performed within 1 visit.

The merged volumetric angiograms were then exported for custom processing using the Center for Ophthalmic Optics & Lasers-Angiography Reading Toolkit software, which removes flow projection artifacts and calculates reflectance-compensated vessel density (VD). These custom programs were developed at the Casey Eye Institute using the MATLAB (Mathworks Inc, Natick, MA) programming language. The OCTA scans contain both volumetric flow (decorrelation) data and structural (reflectance) data. The PR-OCTA algorithm retains flow signal from real blood vessels while suppressing projected flow signal in deeper layers, which appears as downward tails on cross-sectional angiograms and duplicated vascular patterns on en face angiograms.[23,27] Projection-resolved OCTA could visualize up to 4 retinal plexuses: the radial peripapillary capillary plexus (RPCP), the superficial vascular plexus (SVP), the intermediate capillary plexus (ICP), and the deep capillary plexus (DCP).[23,28–31] In the temporal portion of the macula, the RPCP (residing in the NFL) is very thin and cannot be distinguished from the SVP; therefore, we combine the RPCP and the SVP into the superficial vascular complex (SVC). Four en face OCTA slabs were analyzed for VD measurement: SVC, ICP, DCP, and all-plexus retina (SVC + ICP + DCP) (Fig 1). Segmentation of the retinal layers was done by automated MATLAB programs that operate on the structural OCT data. An en face angiogram of each slab was obtained by maximum flow (decorrelation value) projection. The VD, defined as the percentage area occupied by the large vessels and microvasculature, was evaluated in the entire 6×6−mm scan area excluding of the foveal avascular zone (FAZ), which was defined as a 0.6-mm diameter circle centered at the FAZ. The GCC thickness was averaged over the same region. Superior and inferior hemispheric averages were obtained by dividing the scan area across the horizontal meridian.

Because we found VD to be strongly correlated with signal strength index in previous studies, we developed a reflectance-adjustment method that corrected the artifactually lower flow signal in regions of reduced reflectance (e.g., due to media opacity or pupil vignetting).[32] The method is based on statistical analysis of the relationship between the flow noise in the FAZ with reflectance in retinal tissue, in which the reflectance was manipulated by simulated media opacity (optical filters). In the extrafoveal

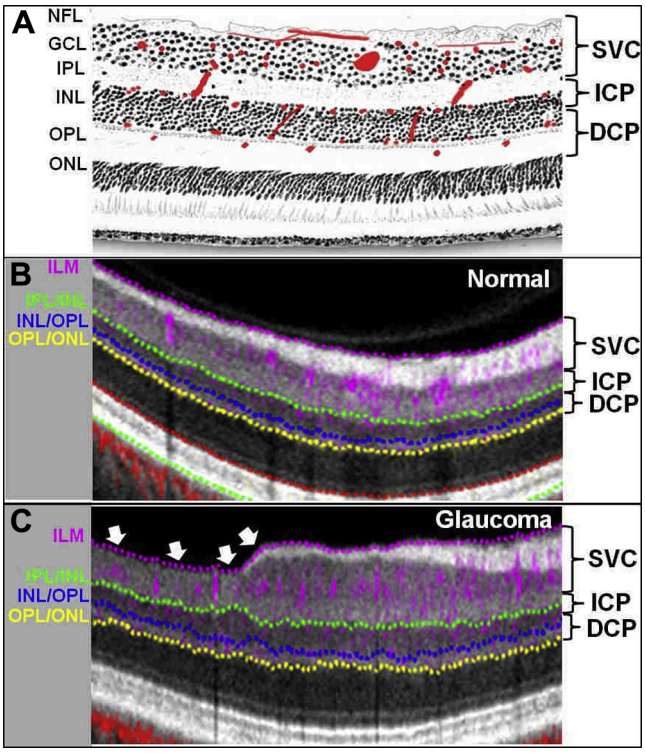

Figure 1. Relationship between the retinal vascular plexuses and the anatomic layers. **A**, The retinal vascular plexuses in red (*right*) hand drawn on top of a histologic section of the human retina showing anatomic layers (*left*). The superficial vascular complex (SVC) supplies most of the ganglion cell complex (GCC). The intermediate capillary plexus (ICP) straddles the inner plexiform layer (IPL) and inner nuclear layer (INL). The deep capillary plexus (DCP) straddles the INL and outer plexiform layer. **B**, Cross-sectional projection-resolved optical coherence tomography angiograms (PR-OCTA) of a normal eye. The 6-mm section is taken 750 μm superior to the fovea. Flow signals (*purple* for retinal and *red* for choroidal blood flow) were overlaid on reflectance signal (*grayscale*). **C**, Projection-resolved OCTA cross-section from a perimetric glaucomatous eye. Focal thinning of nerve fiber layer (NFL) and ganglion cell layer (GCL) could be visualized temporally in the glaucomatous eye (*arrows*), corresponding with the loss of capillaries in the SVC. DCP = deep capillary plexus (outer 50% of INL + outer plexiform layer); GCC (NFL + GCL + IPL) = ganglion cell complex; GCL = ganglion cell layer; ICP = intermediate capillary plexus (outer 20% of the GCC + inner 50% of INL); ILM = inner limiting membrane; INL = inner nuclear layer; IPL = inner plexiform layer; NFL = nerve fiber layer; ONL = outer nuclear layer; OPL = outer plexiform layer; SVC = superficial vascular complex (inner 80% of the GCC).

retina, the average reflectance in the inner nuclear, outer plexiform, and outer nuclear layers to adjust the threshold flow signal value used to classify vessel versus static tissue on en face OCTA. Reflectance compensation is another aspect of the OCTA technique that can be used with PR-OCTA or non−PR-OCTA. Clinical validation showed that this algorithm was able to remove the dependence of retinal VD measurements on OCT signal strength index and reduce population variation.[32]

Image quality was assessed for all OCTA scans. Poor-quality scans with signal strength index below 50 or registered image sets with residual motion artifacts (discontinuous vessel pattern) were excluded from analysis. Two image sets, each meeting the quality criteria, were required to be included in the analysis.

Within-visit repeatability of the VD was calculated with 2 sets of scans performed within a single visit. Within-visit repeatability and population variation were assessed by the coefficient of variation (CV).

All eyes from the glaucoma and normal groups were qualitatively graded for the presence of capillary dropout on the en face OCTA of the SVC, ICP, and DCP slabs (Supplementary material available online at www.aaojournal.org). Only the first merged OCTA from the first set of scan was used in the qualitative grading. The second set was not graded. The grader is a fellowship-trained glaucoma specialist. A training set of macular angiograms of each plexus (SVC, ICP, and DCP) were used to train the grader. The training set was obtained from 5 normal and 5 glaucomatous participants who were not included in the primary analysis. The grader was masked to the identity, clinical information, and glaucoma status of the participant.

Statistical Analysis

Pearson correlation was used to investigate the effect of age, mean ocular perfusion pressure (MOPP), and IOP on VD measurements. MOPP = 2/3*mean arterial pressure − IOP, where mean arterial pressure = 2/3*diastolic blood pressure + 1/3*systolic blood pressure. The Student *t* test was used to compare normal and glaucoma groups. Pearson correlation was used to determine the relationships between macular VD and the traditional glaucoma measurements of function and structure, such as the average retinal sensitivity over the corresponding VF points (central 16 points) and GCC thickness in the glaucoma group. The decibel values for the retinal sensitivity points in the Humphrey Field Analyzer 24-2 test were converted to a linear scale (1/Lambert unit) using the expression $10^{0.1 \times \text{decibel value}}$ and then averaged over hemispheres or the whole eye. The SVC VD value and GCC thickness from that worse hemisphere (superior or inferior) was used to calculate the worse hemisphere diagnostic power. The worse hemisphere has lower fractional deviation from normal. The fractional deviation being the value from the eye under evaluation minus the average of the normal group, then divided by the normal average. Generalized linear model was used to evaluate the effect of eye drops and other factors on the macular VD. All statistical analyses were performed with SPSS 20.0 (SPSS Inc, Chicago, IL) and MedCalc 10.1.3.0 (MedCalc Software, Ostend, Belgium, www.medcalc.be). The area under the receiver operating characteristic curve (AROC), sensitivity, and specificity are used to evaluate diagnostic accuracy. McNemar test and the method of DeLong et al[33] were used to compare sensitivity and AROC of different parameters. The odds ratio test was performed for the qualitative grading results. The statistical significance was assumed at $P < 0.05$. However, for multiple comparisons among the 5 parameters (SVC VD, ICP VD, DCP VD, all-plexus VD, and GCC thickness) measured by OCTA, a Bonferroni correction was applied with resultant significance level set at $P < 0.01$. All OCT and OCTA parameters had normal distributions according to the Shapiro−Wilk test.

Results

Study Population

Macular perfusion was studied in 30 normal and 33 perimetric glaucoma participants. Three glaucoma participants were not analyzed because of poor OCTA scan quality, leaving 30 for statistical analysis. The 30 normal participants provided age-matched comparison with the 30 glaucoma participants (Table 1). Nine participants had mild glaucoma (stage 0−1), 15 participants had moderate glaucoma (stage 2−3), and 6 participants had advanced

Table 1. Participant Characteristics

Parameter	Normal	Glaucoma	Difference (P Value)
Participants, n	30	30	
Eyes, n	30	30	
Age (yrs)	65±9	65±10	
Glaucoma drops, n (%)	0 (0%)	28 (93%)	
IOP (mmHg)	15.1±3.0	14.9±3.1	0.2 (0.609)
Diastolic blood pressure (mmHg)	78.2±11.2	78.8±10.8	−0.6 (0.815)
Systolic blood pressure (mmHg)	125.3±16.9	124.5±17.0	0.8 (0.850)
MOPP (mmHg)	49.0±7.6	47.8±6.6	1.2 (0.782)
VF			
MD (dB)	0.27±1.10 (−3.22∼1.87)	−5.32±3.50 (−13.2∼0.58)	5.59 (<0.001)
PSD (dB)	1.41±0.22 (1.02∼1.85)	6.80±3.70 (1.96∼14.46)	−5.39 (<0.001)
Macular structure			
GCC thickness (μm)	99.8±5.7 (87.0∼111.3)	80.4±10.9 (58.0∼99.0)	19.4 (<0.001)
Macular retinal vessel density (% area)			
SVC	60.5±4.0 (51.2∼68.2)	47.2±7.1 (31.3∼60.5)	13.3 (<0.001)
ICP	38.4±5.9 (29.6∼48.6)	36.3±4.7 (28.0∼46.7)	2.1 (0.133)
DCP	26.3±5.7 (17.3∼38.0)	24.2±7.0 (12.7∼40.4)	2.1 (0.197)
All-plexus	83.2±4.2 (72.5∼89.6)	73.5±6.6 (53.2∼84.2)	9.7 (<0.001)

dB = decibels; DCP = deep capillary plexus; GCC = ganglion cell complex; ICP = intermediate capillary plexus; IOP = intraocular pressure; MD = mean deviation; MOPP = mean ocular perfusion pressure; PSD = pattern standard deviation; SVC = superficial vascular complex; VF = visual field. Numbers displayed are mean ± standard deviation (range).

glaucoma (stage 4–5) glaucoma, according to Glaucoma Staging System 2.[34] A total of 26 participants had primary open-angle glaucoma, 3 participants had low-tension glaucoma, and 1 participant had pigmentary glaucoma. There was no statistically significant difference between the normal and glaucoma groups for age, IOP, MOPP, and systolic/diastolic blood pressure (Table 1).

Qualitative Assessment of Focal Capillary Dropout

In the normal eye (Fig 2), the en face PR-OCTA of the SVC in the macula shows centripetally branching vessels, terminating in the central FAZ. The VD is higher nasally, corresponding to the thicker NFL near the optic disc. The ICP and DCP are pure capillary layers of uniform vessel caliber and density, with the exception of the FAZ. The normal GCC is thickest in the parafoveal annulus, but absent in the fovea itself. The PR-OCTA and non–PR-OCTA SVC angiograms were identical, as would be expected because this is the most superficial layer and thus should be devoid of projection artifacts. Non–PR-OCTA angiograms showed vessel patterns in the SVC are duplicated in the ICP and DCP. The majority of artifactual duplication from the SVC were absent in PR-OCTA ICP and DCP angiograms. A perimetric glaucoma eye with a well-defined arcuate defect was chosen to demonstrate the regional correspondence between VD, GCC thickness, and VF (Fig 3). Severe capillary dropout could be visualized in the SVC within the arcuate defect, whereas the ICP and DCP were not visibly affected in PR-OCTA angiograms. However, focal defects and vessel patterns from the SVC are clearly projected in the ICP and DCP in non–PR-OCTA angiograms. Cross-sectional OCTA of the same eye (Fig 1) also demonstrated the correspondence between GCC thinning and loss of capillaries in the SVC. The all-plexus angiogram (Fig 3), which includes the SVC, ICP, and DCP, showed only a mild decrease in VD in the area of the arcuate defect. Thus, the SVC slab provided the best contrast for visualizing focal glaucomatous defects on en face PR-OCTA. The GCC map showed thinning in the same area as the SVC capillary dropout. The VF pattern deviation map shows an inferior arcuate defect matching the location of the SVC and GCC defects.

A masked qualitative grading was performed on en face OCTA of the SVC, ICP, and DCP separately. In the SVC angiograms, 27 (90%) glaucomatous eyes and 4 (13%) normal eyes were identified as having areas of capillary dropout. The ratios were significantly different ($P < 0.001$). In the ICP angiograms, 16 (53%) glaucomatous eyes and 5 (16%) normal eyes were graded as having capillary dropout. The ratios were significantly different ($P = 0.004$). In the DCP angiograms, 5 (16%) glaucomatous eyes and 6 (20%) normal eyes were graded as having capillary dropout. The ratios were similar ($P = 0.52$).

Correlation of Optical Coherence Tomography Angiography and Structural Optical Coherence Tomography Parameters with Clinical Variables

After the application of the Bonferroni correction for multiple comparisons, the SVC VD, all-plexus VD, and GCC thickness in the glaucoma group were significantly lower than in the normal group (all $P < 0.001$, t test). The VD of the deeper plexuses (ICP and DCP) in the glaucoma group was not significantly lower than in the normal group (Table 1). In the normal group, the all-plexus VD and ICP VD were both correlated with age: $r = -0.467$, $P = 0.009$, all-plexus VD = (−0.22*age + 97.6)*100%; $r = -0.539$, $P = 0.002$, ICP VD = (−0.107*age + 67.5)*100%.

Four classes of glaucoma drops were used in 29 eyes. Prostaglandin analogs were used in 26 eyes. β-blockers were used in 10 eyes. Alpha agonists were used in 6 eyes. Topical carbonic anhydrase inhibitors were used in 15 eyes. Because SVC is the most relevant slab to glaucoma damage, a generalized linear model was performed to evaluate the correlation between glaucoma drops and SVC VD. The eyes with β-blocker use had 3.3% lower macular SVC VD ($P = 0.043$), after adjusting for macular GCC thickness.

Repeatability and Population Variation

In both normal and glaucoma participants, the SVC/all-plexus VD and GCC thickness all had excellent within-visit repeatability (Table 2). In comparison, the repeatability of ICP and DCP VD was significantly worse ($P < 0.025$, Wilcoxon signed-rank test). The

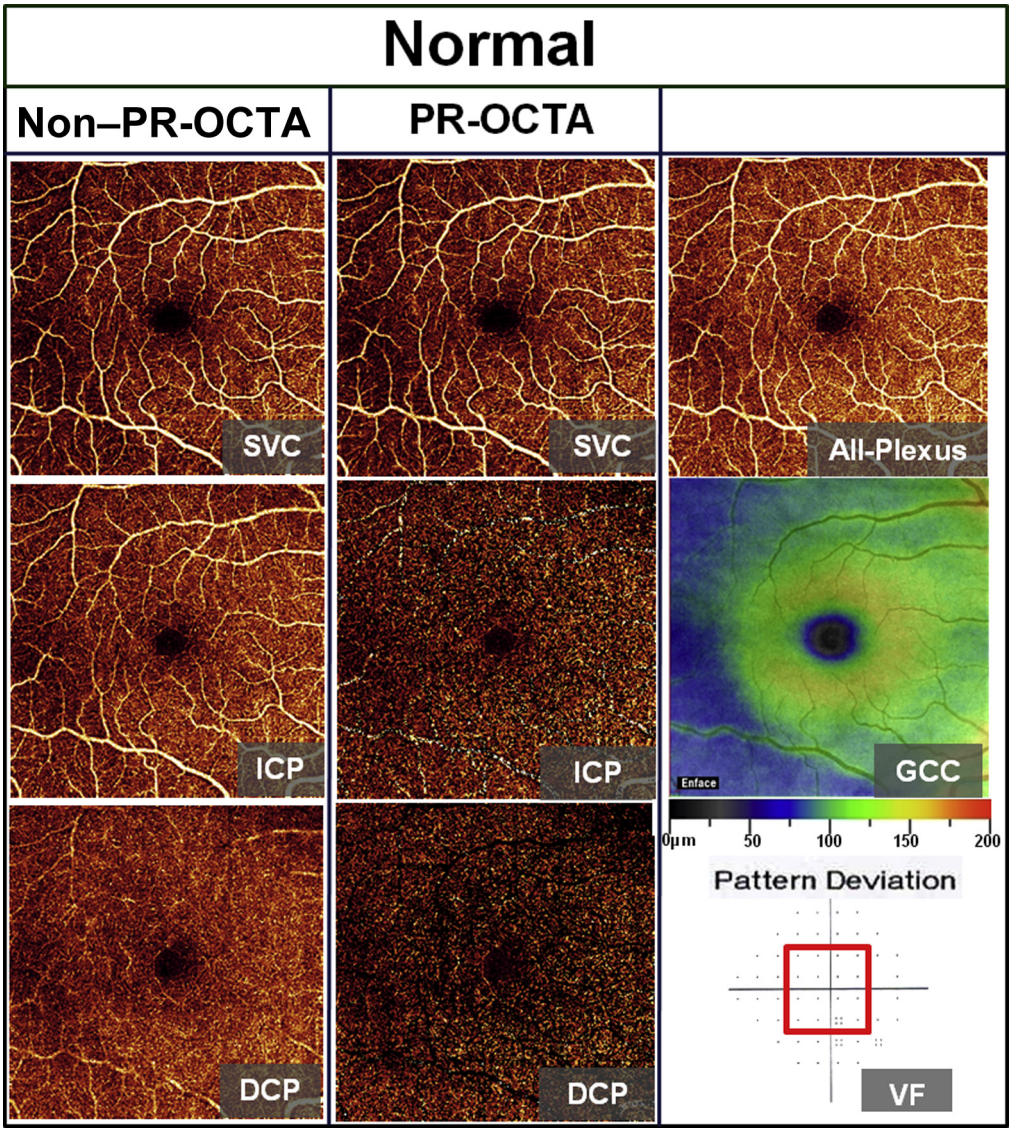

Figure 2. The 6×6−mm en face angiograms of a normal eye shown were from non−projection-resolved optical coherence tomography angiography (PR-OCTA) (*first column*) and PR-OCTA (*second column*). The central 16 points (±10° enclosed in *red line*) of the Humphrey 24-2 visual field (VF) pattern deviation map approximately corresponds to the area of the 6×6−mm PR-OCTA and ganglion cell complex (GCC) thickness maps.[11] The vessel pattern in the superficial vascular complex (SVC) is duplicated in the non−PR-OCTA intermediate capillary plexus (ICP) and deep capillary plexus (DCP) angiograms. The majority of the projection artifacts were absent in the PR-OCTA ICP and DCP angiograms.

SVC VD, all-plexus VD, and GCC thickness all had tight population variation. In comparison, ICP and DCP VD had wider population variation, but the difference was not statistically significant.

Glaucoma Diagnostic Accuracy

The overall SVC VD had the best diagnostic accuracy among the global parameters, as judged by the sensitivity and area under the receiver operating curve (AROC) for differentiating normal and glaucoma eyes (Table 3). However, it did not differ significantly with all-plexus VD and GCC thickness AROCs ($P > 0.109$). Likewise, parameters in the worse hemisphere had even higher diagnostic accuracy than the global parameters, but again the superiority was not statistically significant when comparing the SVC, all-plexus VD, and GCC thickness. The best diagnostic accuracy was obtained with the SVC VD in the worse hemisphere, which had an AROC of 0.983 and a sensitivity of 96.7% at a fixed specificity of 95%.

Correlation with Traditional Glaucoma Diagnostic Measurements

In the glaucoma group, the overall SVC VD had excellent correlation with the GCC thickness and good correlation with the VF sensitivity averaged within the corresponding central 16 points (Table 4). These correlations were highly significant. The overall all-plexus VD did not correlate as well with GCC and had no significant correlation with VF. When the SVC VD and GCC thickness were divided into hemispheres, they had even higher correlation with VF sensitivity in the corresponding hemisphere (Table 5). This correlation was region specific, because there was no correlation with the noncorresponding hemisphere.

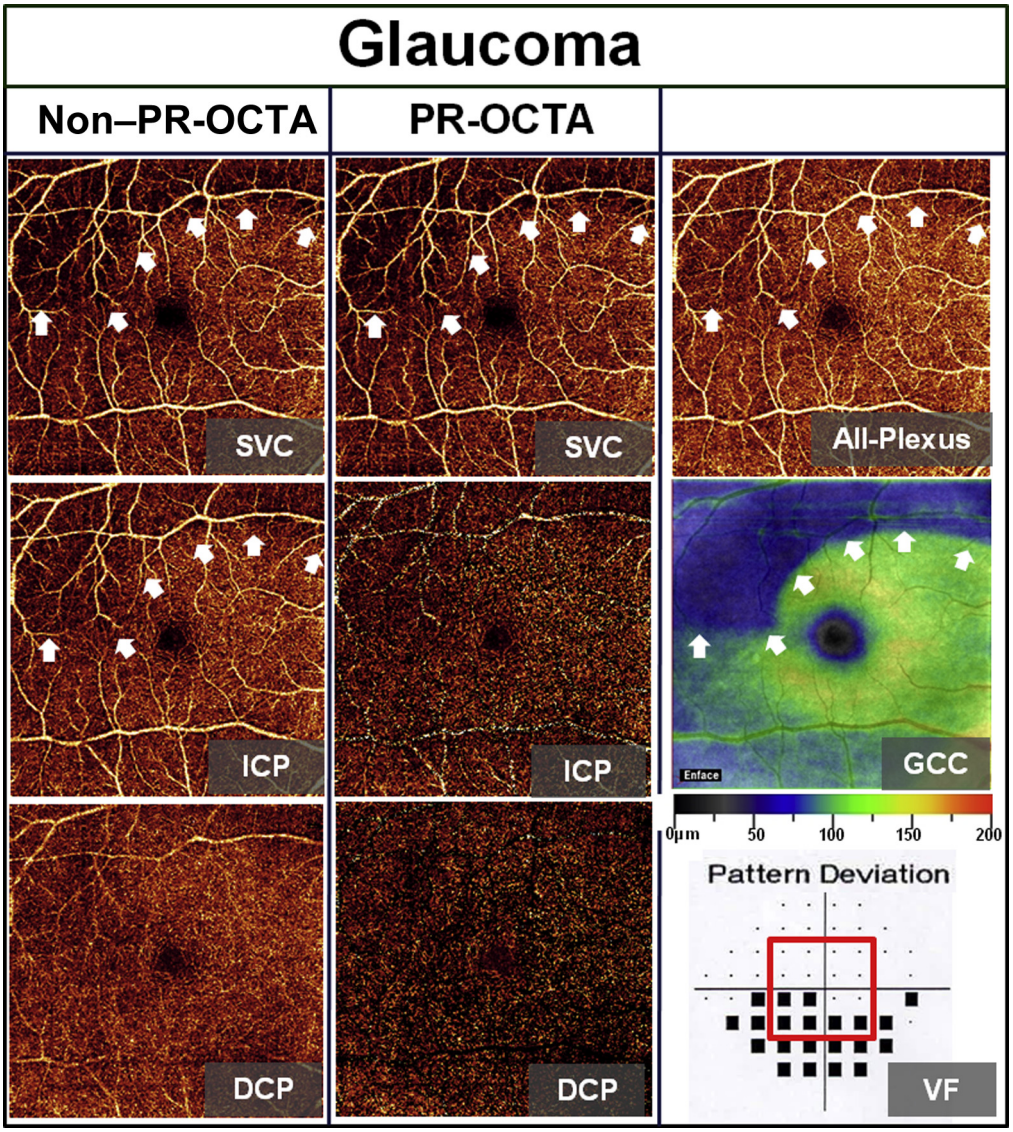

Figure 3. The 6×6−mm en face angiograms of a perimetric glaucoma eye shown were from non−projection-resolved optical coherence tomography angiography (PR-OCTA) (*first column*) and PR-OCTA (*second column*). The glaucomatous eye has a superior arcuate defect (*arrows*) appearing as focal decrease of vessel density (VD) on the PR-OCTA of the superficial vascular complex (SVC) and all-plexus slabs, as well as focal thinning on the ganglion cell complex (GCC) map. They correspond to the inferior visual field (VF) defect (bottom 6 *black squares* within the *red outlined* area). The focal defects in the SVC are clearly projected in the non−PR-OCTA ICP angiogram (*arrows*). DCP = deep capillary plexus; ICP = intermediate capillary plexus.

Correlation of Vessel Density with Stage of Glaucoma

In the glaucoma group, both SVC VD ($r = -0.369$, $P = 0.045$) and GCC thickness ($r = -0.410$, $P = 0.025$) were significantly correlated with glaucoma stage, as determined by the enhanced Glaucoma Staging System.[34] The all-plexus VD, ICP VD, and DCP VD did not have a statistically significant correlation with glaucoma stages.

Role of Reflectance Compensation in Vessel Density Measurements

The VD values shown are compensated for retinal reflectance variation using a previously published method to adjust the threshold decorrelation value for distinguishing vessel from static tissue according to the local retinal reflectance value.[32] To demonstrate the importance of this reflectance compensation method, we also calculated the SVC VD using a fixed threshold that does not compensate for reflectance variation. In normal participants, the population variation of the reflectance-adjusted macular SVC VD was 6.6% CV, which was smaller ($P = 0.013$, F test) than the variation without reflectance adjustment (9.7% CV). The repeatability of the reflectance-adjusted SVC VD was 1.8% CV, which was better (0.002, Wilcoxon signed-rank test) than the repeatability without reflectance adjustment (3.8% CV). The SVC VD without reflectance adjustment was correlated with signal strength index (Pearson $r = 0.731$, $P < 0.001$), whereas the reflectance-adjusted SVC VD was independent from signal strength index (Pearson $r = 0.107$, $P = 0.416$). The AROC was 0.961 for the reflectance-adjusted SVC VD, which was not significantly better than the AROC

Table 2. Repeatability and Normal Population Variability of Macular Parameters

Group	Normal		Glaucoma
Parameter	Within-Visit Repeatability (CV)	Population Variation (CV)	Within-Visit Repeatability (CV)
SVC VD	1.8%	6.6%	3.0%
ICP VD	5.6%	15.4%	7.4%
DCP VD	8.4%	21.7%	10.5%
All-plexus VD	1.7%	5.0%	2.4%
GCC thickness	1.2%	5.7%	1.9%

CV = coefficient of variation; DCP = deep capillary plexus; GCC = ganglion cell complex; ICP = intermediate capillary plexus; SVC = superficial vascular complex; VD = vessel density.

(0.933) for the SVC VD without reflectance adjustment. When the specificities were fixed at 95%, the sensitivities were the same (80%) for the 2 methods. In the glaucoma group, there was no correlation between the SVC VD without reflectance adjustment and the corresponding VF points (Pearson $r = 0.186$, $P = 0.326$). After the reflectance compensation, the SVC VD correlated well with the corresponding VF points (Pearson $r = 0.444$, $P = 0.014$) (Fig 4). The reflectance adjustment appears to reduce the spread (noise) in VD values and therefore improved the correlation with VF sensitivity. The reflectance compensation also improved the correlation between SVC VD and GCC thickness (from Pearson $r = 0.616$ to 0.804, both $P < 0.001$).

Discussion

Studies using OCTA have shown that glaucoma reduces perfusion in the optic nerve head and the peripapillary retina.[14–19] But the 6×6−mm macular region has not been studied with this new imaging technology. Because glaucoma damages RGCs and approximately one third of RGCs reside in the macula, macular perfusion is theoretically a good place to detect glaucoma and assess disease severity.[4,5] Structural OCT studies have shown that the macular GCC thickness and other measures of RGC volume are reduced in patients with glaucoma,[6–8] and focal loss of macular GCC is a good predictor of VF conversion and progression.[13] Measuring the macular perfusion has the potential for detecting reduced metabolic rate in dysfunctional in RGCs before they undergo apoptosis and cause the GCC to become thinner. This study aimed to evaluate whether macular VD, as measured by OCTA, is decreased in glaucomatous eyes, and if so, to characterize the regional correlation with VF and structural OCT parameters.

To better characterize the location of decreased perfusion in glaucomatous eyes, we used a "projection-resolved" algorithm to remove flow projection artifacts.[23] This algorithm allowed us to separately analyze the retinal circulation in 3 layers: SVC, ICP, and DCP. We found that glaucoma affected the SVC to a greater degree than the deep vascular complex (DVC, comprising the ICP and DCP). This was shown by both qualitative grading of focal capillary dropout and automated quantitative VD measurements. It is not surprising that the SVC VD was greatly reduced in glaucomatous eyes because it supplies the NFL, GCL, and part of the IPL,[28–30] the anatomic layers most affected by glaucoma.[6,8–10] The ICP also partly supplies the IPL, but its density was only slightly reduced by glaucoma in this study. The DCP was minimally affected by glaucoma, because it supplies the middle retinal layers that do not include the RGCs.

Although the PR-OCTA algorithm aids in removing flow projection artifacts, it does not do so perfectly. The en face OCTA of the ICP and DCP still show some residual projection and shadow artifacts that are visible under large retinal vessels in the SVC. However, the repeatability of the overall VDs in all of the plexuses were all acceptable. We were able to show that ICP and DCP are mostly preserved in glaucomatous eyes, which suggests that PR-OCTA was effective in removing most of the projection artifacts. If conventional OCTA were used, one would see a duplication of SVC vascular patterns in the deeper retinal layers, including the ICP and DCP slabs,[23,35–38] and this would have led to an erroneous impression that ICP and DCP are also affected by glaucoma. However, for glaucoma evaluation, both PR-OCTA and non−PR-OCTA will work because SVC is the preferential affected layer, and there is no projection artifact in this most superficial layer.

Although the DVC was only minimally reduced in glaucoma, it is not clear a priori whether combining it with the SVC to obtain measurement of the all-plexus retinal circulation would aid or hinder the diagnosis of glaucoma. However, including the DVC in VD measurement might introduce noise from tissue unaffected by glaucoma. On the other hand, segmentation of the all-plexus retinal slab is easier than segmentation of the narrower SVC slab and

Table 3. Diagnostic Accuracy of Macular Optical Coherence Tomography Parameters

Parameters	AROC	Sensitivity
Overall SVC VD	0.961	80.0%
Overall all-plexus VD	0.906	70.0%
Overall GCC thickness	0.950	76.7%
Worse hemisphere SVC VD	0.983	96.7%
Worse hemisphere GCC thickness	0.973	86.7%

AROC = area under the receiver operating characteristic curve; GCC = ganglion cell complex; SVC = superficial vascular complex; VD = vessel density.
Sensitivities at 95% specificity were evaluated.

Table 4. Correlation Matrix of Macular Parameters in Glaucoma Participants

Parameters	SVC VD	All-Plexus VD	GCC Thickness
All-plexus VD	**0.696 (0.000)**		
GCC thickness	**0.804 (0.000)**	**0.435 (0.016)**	
VF retinal sensitivity*	**0.444 (0.014)**	0.186 (0.326)	**0.450 (0.013)**

GCC = ganglion cell complex; SVC = superficial vascular complex; VD = vessel density; VF = visual field.
Pearson's r (P value). Statistically significant correlations ($P < 0.05$) are boldfaced.
*The VF retinal sensitivity values were converted from decibels to 1/Lambert.

Table 5. Correlation of Hemisphere Macular Parameters in Glaucoma Participants

Parameters	Superior VF Retinal Sensitivity*	Inferior VF Retinal Sensitivity*	Superior GCC Thickness	Inferior GCC Thickness
Superior SVC VD	0.063 (0.739)	**0.530 (0.003)**	**0.827 (0.000)**	0.284 (0.128)
Inferior SVC VD	**0.689 (0.000)**	0.082 (0.668)	0.299 (0.109)	**0.845 (0.000)**

GCC = ganglion cell complex; SVC = superficial vascular complex; VD = vessel density; VF = visual field.
Pearson's r (P value to test $|R| = 0$). Statistically significant correlation ($P < 0.05$) are boldfaced.
*The VF retinal sensitivity values were converted from decibels to 1/Lambert.

might provide more robust results. Our results showed that although the all-plexus retinal VD was slightly more repeatable than SVC-VD, the diagnostic accuracy was better using the SVC-VD. Although the difference in diagnostic accuracy was not statistically significant because of the limited sample size, we were able to further demonstrate that SVC-VD was significantly better correlated with VF sensitivity in the macular test points. Thus, for the purpose of glaucoma assessment, it is advantageous to assess the SVC perfusion and exclude the DVC.

Qualitative grading of SVC angiograms also showed good sensitivity (90%) and specificity (87%) for distinguishing glaucomatous and normal eyes. Thus, even in the absence of automated diagnostic parameters in commercial OCTA systems, the clinician could already use the en face SVC angiogram to visualize capillary dropout and evaluate glaucoma damage. There is a need to develop automated software to identify areas with reduced capillary perfusion, which could improve the evaluation of focal glaucoma damage.

The SVC VD in the worse hemisphere (superior or inferior) had excellent diagnostic accuracy with an AROC of 0.983 and a sensitivity of 96.7% at 95% specificity. This compares favorably with the diagnostic accuracy in studies that used structural OCT parameters for diagnosis in comparable groups of perimetric glaucoma subjects (mostly early to moderate stage).[6,8,38] Our sample size of 30 participants with glaucoma and 30 normal participants would be able to detect an only statistically significant difference from an AROC of 0.983 if the comparative AROC were 0.900 or less. Thus, we are not able to detect a significant difference in diagnostic accuracy between OCTA and structural OCT parameters. A larger study with higher statistical power is needed to compare OCTA and structural OCT in the diagnosis of glaucoma.

The diagnostic accuracy of macular OCTA was studied by Rao et al[22] in comparison with peripapillary and disc OCTA. In sharp contrast to our results, they found that macular VD had poor diagnostic accuracy (AROC = 0.69), significantly worse than that of the whole disc/peripapillary region (AROC = 0.90). Our higher diagnostic accuracy was most likely due to a larger macular scan area of 6×6−mm compared with the small scan area of 3×3 mm used by Rao et al.[22] The macular area that is most vulnerable to glaucoma is inferior and inferotemporal, lying mostly outside the central 3×3−mm area.[11] We further improved AROC by measuring the VD in the SVC and compensating for variation in OCT signal strength. The glaucoma populations in the 2 studies were similar in terms of the severity of VF damage as summarized by mean deviation.

In our previous study, we noticed that OCTA flow signals were affected by the structural OCT reflectance signal strength. Vessels under vitreous opacities appeared fainter on OCTA, and eyes with lower signal strength index tended to have lower retinal VD. We developed a method to adjust for the effect of reflectance on VD.[32] This algorithm effectively removes the dependence of VD on the signal strength index. However, it was not known a priori whether the reflectance adjustment would aid or hinder glaucoma diagnostic accuracy. On the one hand, the reflectance adjustment could provide more

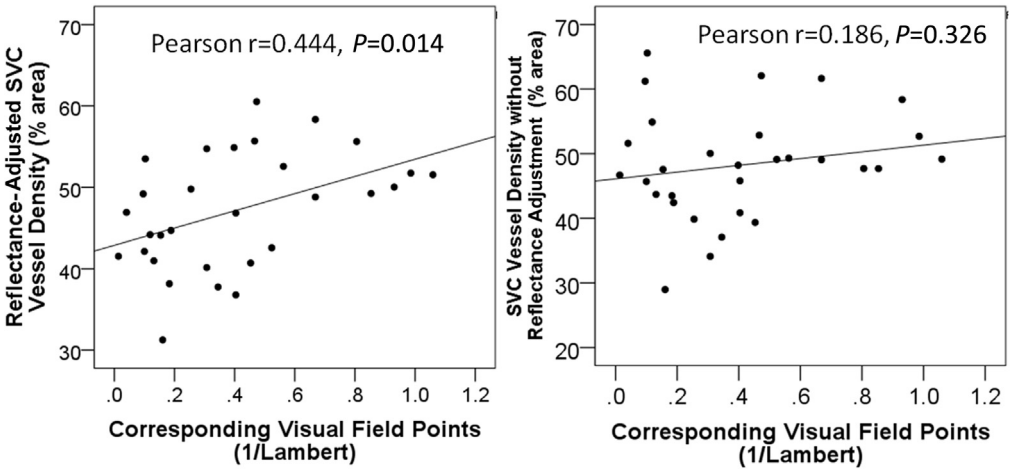

Figure 4. Plots of reflectance-adjusted superficial vascular complex (SVC) vessel density (VD) versus corresponding VF retinal sensitivity (*left*) and SVC VD without reflectance adjustment versus corresponding VF retinal sensitivity (*right*).

accurate VD measurements by removing variability due to factors that affect signal strength (media opacity, pupil vignetting, defocus). On the other hand, the glaucomatous retina might have lower tissue reflectivity and adjusting for reflectance might remove this contributory diagnostic information. Our results empirically demonstrated that reflectance adjustment significantly improved the repeatability of the SVC VD measurements in both normal and glaucoma groups, as well as reduced the normal population variation. Reflectance adjustment also improved glaucoma diagnostic accuracy, but statistical significance could not be demonstrated because of the small sample size. The importance of using the reflectance-adjusted VD became clear when evaluating the association between SVC VD and VF defects. Without the reflectance adjustment, there was no significant association between SVC VD and retinal sensitivity in the corresponding VF points. With the reflectance adjustment, there was a significant association between SVC VD and retinal sensitivity (Fig 4), indicating that it improved the measurement of disease severity. Overall, our results indicate that reflectance adjustment is helpful when using macular OCTA to evaluate glaucoma.

Currently, VF testing remains the gold standard for assessing glaucoma severity and progression.[39] However, patients often have difficulty taking a VF test and undergoing a lengthy procedure, and repeatability is a problem with this subjective test.[40,41] In contrast, both SVC VD with reflectance adjustment and GCC thickness data provide quick, objective data that show excellent correlation with VF measures and disease severity. Thus, SVC VD and GCC thickness data may be well positioned to provide an objective, quantitative measure of glaucoma severity. Our results did not show SVC VD to be superior to GCC thickness in terms of diagnosis of glaucoma and correlation with VF, which may limit clinical utility. However, the 2 parameters may be complementary and further studies will be needed. The excellent reproducibility of SVC VD and GCC thickness suggests that they may offer a precise way of monitoring disease progression. Further longitudinal studies are warranted.

Hand in hand with the need for further longitudinal studies is the need for further age-adjusted normative data on OCTA paramenters.[42] Our data suggest that all-plexus VD in normal participants may decline with age at a rate of approximately 0.2% per year. This number is remarkably similar to the age-related rate of GCC and NFL thinning found in a recent longitudinal study of OCT structural parameters,[43] raising the intriguing possibility that the age-related decline in both retinal VD and thickness may be aspects of the same process. However, the small sample size and cross-sectional nature of our current study preclude making any definitive conclusions.

Study Limitations

A limitation of this study was that patients with pre-perimetric glaucoma and glaucoma suspects were not included. Therefore, we could not draw conclusions concerning diagnostic accuracy in the earliest stages of glaucoma.

Our study also found an association between β-blocker eye drop use and decreased macular SVC VD. The causative explanation could be that β-blockers have a direct vasoconstrictive effect that decreased VD, which would have implications on the use of β-blocker eye drops compared with a choice of other glaucoma medications. However, we cannot yet conclude that β-blockers caused a reduction in blood flow because the regression analysis could be affected by selection bias. Although we have already adjusted for the effect of glaucoma severity by using GCC thickness as a covariate in the analysis, we cannot completely rule out the possibility that participants with worse glaucoma, and thus decreased SVC VD, may be more likely to be using a β-blocker. Further prospective investigations of glaucoma drop use on ocular perfusion are needed. In any case, the β-blocker effect is too small to account for the dramatically decreased SVC VD that we identified in patients with glaucoma that is clearly due to glaucoma damage given the high correlation with the severity and location of VF and GCC defects.

In summary, we showed that OCTA evaluation of the macula could measure VD with high repeatability and detect glaucoma damage with high sensitivity. Focusing the VD analysis to the SVC slab and the use of a reflectance-compensation method to reduce the effect of signal strength variation appeared to enhance glaucoma diagnostic accuracy and correlation with disease severity as measured by VF and GCC thickness. Both SVC VD and GCC thickness correlated well with VF and may work synergistically to serve as an objective alternative for central VF assessment in glaucoma diagnosis and monitoring. Several OCT companies have introduced OCTA products that could assess perfusion in the macular and optic nerve regions. We hope the results presented in this article will motivate and guide further investigations of OCTA in glaucoma evaluation.

References

1. Quigley HA, Broman AT. The number of people with glaucoma worldwide in 2010 and 2020. *Br J Ophthalmol*. 2006;90:262-267.
2. Leske MC. Open-angle glaucoma—an epidemiologic overview. *Ophthalmic Epidemiol*. 2007;14:166-172.
3. Congdon NG, Friedman DS, Lietman T. Important causes of visual impairment in the world today. *JAMA*. 2003;290:2057-2060.
4. Quigley HA, Dunkelberger GR, Green WR. Retinal ganglion cell atrophy correlated with automated perimetry in human eyes with glaucoma. *Am J Ophthalmol*. 1989;107:453-464.
5. Curcio CA, Allen KA. Topography of ganglion cells in human retina. *J Comp Neurol*. 1990;300:5-25.
6. Tan O, Chopra V, Lu AT, et al. Detection of macular ganglion cell loss in glaucoma by Fourier-domain optical coherence tomography. *Ophthalmology*. 2009;116:2305-2314.e1-e2.
7. Tan O, Li G, Lu AT, et al. Mapping of macular substructures with optical coherence tomography for glaucoma diagnosis. *Ophthalmology*. 2008;115:949-956.
8. Mwanza JC, Durbin MK, Budenz DL, et al. Glaucoma diagnostic accuracy of ganglion cell-inner plexiform layer thickness: comparison with nerve fiber layer and optic nerve head. *Ophthalmology*. 2012;119:1151-1158.
9. Burgansky-Eliash Z, Wollstein G, Chu T, et al. Optical coherence tomography machine learning classifiers for

glaucoma detection: a preliminary study. *Invest Ophthalmol Vis Sci*. 2005;46:4147-4152.
10. Loewen NA, Zhang X, Tan O, et al. Combining measurements from three anatomical areas for glaucoma diagnosis using Fourier-domain optical coherence tomography. *Br J Ophthalmol*. 2015;99:1224-1229.
11. Hood DC, Raza AS, de Moraes CG, et al. Glaucomatous damage of the macula. *Prog Retin Eye Res*. 2013;32:1-21.
12. Traynis I, De Moraes CG, Raza AS, et al. Prevalence and nature of early glaucomatous defects in the central 10 degrees of the visual field. *JAMA Ophthalmol*. 2014;132:291-297.
13. Zhang X, Loewen N, Tan O, et al. Predicting development of glaucomatous visual field conversion using baseline Fourier-domain optical coherence tomography. *Am J Ophthalmol*. 2016;163:29-37.
14. Jia Y, Wei E, Wang X, et al. Optical coherence tomography angiography of optic disc perfusion in glaucoma. *Ophthalmology*. 2014;121:1322-1332.
15. Liu L, Jia Y, Takusagawa HL, et al. Optical coherence tomography angiography of the peripapillary retina in glaucoma. *JAMA Ophthalmol*. 2015;133:1045-1052.
16. Yarmohammadi A, Zangwill LM, Diniz-Filho A, et al. Relationship between optical coherence tomography angiography vessel density and severity of visual field loss in glaucoma. *Ophthalmology*. 2016;123:2498-2508.
17. Suh MH, Zangwill LM, Manalastas PI, et al. Optical coherence tomography angiography vessel density in glaucomatous eyes with focal lamina cribrosa defects. *Ophthalmology*. 2016;123:2309-2317.
18. Hollo G. Vessel density calculated from OCT angiography in 3 peripapillary sectors in normal, ocular hypertensive, and glaucoma eyes. *Eur J Ophthalmol*. 2016;26:e42-e45.
19. Lee EJ, Lee KM, Lee SH, Kim TW. OCT angiography of the peripapillary retina in primary open-angle glaucoma. *Invest Ophthalmol Vis Sci*. 2016;57:6265-6270.
20. Rao HL, Pradhan ZS, Weinreb RN, et al. Vessel density and structural measurements of optical coherence tomography in primary angle closure and primary angle closure glaucoma. *Am J Ophthalmol*. 2017;177:106-115.
21. Yarmohammadi A, Zangwill LM, Diniz-Filho A, et al. Peripapillary and macular vessel density in patients with glaucoma and single-hemifield visual field defect. *Ophthalmology*. 2017;124:709-719.
22. Rao HL, Pradhan ZS, Weinreb RN, et al. Regional comparisons of optical coherence tomography angiography vessel density in primary open-angle glaucoma. *Am J Ophthalmol*. 2016;171:75-83.
23. Zhang M, Hwang TS, Campbell JP, et al. Projection-resolved optical coherence tomographic angiography. *Biomed Opt Express*. 2016;7:816-828.
24. Jia Y, Lumbroso B, Gao S, et al. Cross-sectional and en face visualization of posterior eye circulations. In: Huang D, Lumbroso B, Jia Y, Waheed N, eds. *Optical Coherence Tomography Angiography of the Eye*. Thorofare, NJ: Slack Inc. 2017:19-24.
25. Jia Y, Tan O, Tokayer J, et al. Split-spectrum amplitude-decorrelation angiography with optical coherence tomography. *Opt Express*. 2012;20:4710-4725.
26. Kraus MF, Potsaid B, Mayer MA, et al. Motion correction in optical coherence tomography volumes on a per A-scan basis using orthogonal scan patterns. *Biomed Opt Express*. 2012;3:1182-1199.
27. Gao S, Jia Y, Huang D. Artifacts in optical coherence tomography. In: Huang D, Lumbroso B, Jia Y, Waheed N, eds. *Optical Coherence Tomography Angiography of the Eye*. Thorofare, NJ: Slack Inc. 2017:31-38.
28. Snodderly DM, Weinhaus RS, Choi JC. Neural-vascular relationships in central retina of macaque monkeys (*Macaca fascicularis*). *J Neurosci*. 1992;12:1169-1193.
29. Provis JM. Development of the primate retinal vasculature. *Prog Retin Eye Res*. 2001;20:799-821.
30. Snodderly DM, Weinhaus RS. Retinal vasculature of the fovea of the squirrel monkey, *Saimiri sciureus*: three-dimensional architecture, visual screening, and relationships to the neuronal layers. *J Comp Neurol*. 1990;297:145-163.
31. Campbell JP, Zhang M, Hwang TS, et al. Detailed vascular anatomy of the human retina by projection-resolved optical coherence tomography angiography. *Sci Rep*. 2017;7:42201.
32. Gao SS, Jia Y, Liu L, et al. Compensation for reflectance variation in vessel density quantification by optical coherence tomography angiography. *Invest Ophthalmol Vis Sci*. 2016;57:4485-4492.
33. DeLong ER, DeLong DM, Clarke-Pearson DL. Comparing the areas under two or more correlated receiver operating characteristic curves: a nonparametric approach. *Biometrics*. 1988;44:837-845.
34. Brusini P, Filacorda S. Enhanced Glaucoma Staging System (GSS 2) for classifying functional damage in glaucoma. *J Glaucoma*. 2006;15:40-46.
35. Spaide RF, Fujimoto JG, Waheed NK. Image artifacts in optical coherence tomography angiography. *Retina*. 2015;35:2163-2180.
36. Ferrara D. Image artifacts in optical coherence tomography angiography. *Clin Exp Ophthalmol*. 2016;44:367-368.
37. Zhang A, Zhang Q, Wang RK. Minimizing projection artifacts for accurate presentation of choroidal neovascularization in OCT micro-angiography. *Biomed Opt Express*. 2015;6:4130-4143.
38. Mwanza JC, Oakley JD, Budenz DL, Anderson DR. Ability of cirrus HD-OCT optic nerve head parameters to discriminate normal from glaucomatous eyes. *Ophthalmology*. 2011;118:241-248.e1.
39. Sharma P, Sample PA, Zangwill LM, Schuman JS. Diagnostic tools for glaucoma detection and management. *Surv Ophthalmol*. 2008;(53 Suppl 1):S17-S32.
40. Keltner JL, Johnson CA, Anderson DR, et al. The association between glaucomatous visual fields and optic nerve head features in the Ocular Hypertension Treatment Study. *Ophthalmology*. 2006;113:1603-1612.
41. Keltner JL, Johnson CA, Levine RA, et al. Normal visual field test results following glaucomatous visual field end points in the Ocular Hypertension Treatment Study. *Arch Ophthalmol*. 2005;123:1201-1206.
42. Coscas F, Sellam A, Glacet-Bernard A, et al. Normative data for vascular density in superficial and deep capillary plexuses of healthy adults assessed by optical coherence tomography angiography. *Invest Ophthalmol Vis Sci*. 2016;57:OCT211-OCT223.
43. Zhang X, Francis BA, Dastiridou A, et al. Longitudinal and cross-sectional analyses of age effects on retinal nerve fiber layer and ganglion cell complex thickness by Fourier-Domain OCT. *Transl Vis Sci Technol*. 2016;5:1.

Footnotes and Financial Disclosures

Originally received: January 20, 2017.
Final revision: May 23, 2017.
Accepted: June 2, 2017.

Available online: July 1, 2017. Manuscript no. 2016-1061.

Casey Eye Institute and Department of Ophthalmology, Oregon Health and Science University, Portland, Oregon.

Presented in part: the American Glaucoma Society annual meeting, March 3−6, 2016, Fort Lauderdale, Florida; and the Association for Research in Vision and Ophthalmology annual meeting, May 1−5, 2016, Seattle, Washington.

*H.T. and L.L. are co-first authors and contributed equally to this study.

Financial Disclosure(s):
The author(s) have made the following disclosure(s): O.H.S.U., Y.J., and D.H.: Financial interest − Optovue, Inc, a company that may have a commercial interest in the results of this research and technology. These potential conflicts of interest have been reviewed and managed by OHSU.

S.G.: Joined Genentech in January 2017.

M.Z.: Joined Optovue Inc, in July 2016.

Financial support: National Institutes of Health Grants R01 EY023285, P30 EY010572 (Bethesda, MD), an unrestricted departmental funding from Research to Prevent Blindness (New York, NY), and the Antonio Champalimaud Vision Award. The sponsor or funding organization had no role in the design or conduct of this research.

Author Contributions:

Conception and design: Jia, Morrison, Huang

Data collection: Takusagawa, Liu, Ma, Gao, Zhang, Edmunds, Parikh, Tehrani

Analysis and interpretation: Takusagawa, Liu, Ma, Jia, Gao, Zhang, Edmunds, Parikh, Tehrani, Morrison, Huang

Obtained funding: Jia, Morrison, Huang

Overall responsibility: Takusagawa, Liu, Ma, Jia, Huang

Abbreviations and Acronyms:
AROC = area under the receiver operating characteristic curve; **CV** = coefficient of variation; **DCP** = deep capillary plexus; **DVC** = deep vascular complex; **FAZ** = foveal avascular zone; **GCC** = ganglion cell complex; **GCL** = ganglion cell layer; **ICP** = intermediate capillary plexus; **IOP** = intraocular pressure; **IPL** = inner plexiform layer; **MOPP** = mean ocular perfusion pressure; **NFL** = nerve fiber layer; **OCT** = optical coherence tomography; **OCTA** = optical coherence tomography angiography; **OHSU** = Oregon Health & Science University; **PR-OCTA** = projection-resolved optical coherence tomography angiography; **RGC** = retinal ganglion cell; **RPCP** = radial peripapillary capillary plexus; **SVC** = superficial vascular complex; **SVP** = superficial vascular plexus; **VD** = vessel density; **VF** = visual field.

Correspondence:
David Huang, MD, PhD, Casey Eye Institute, Oregon Health & Science University, 3375 SW Terwilliger Boulevard, Portland, OR 97239-4197. E-mail: davidhuang@alum.mit.edu.

Pictures & Perspectives

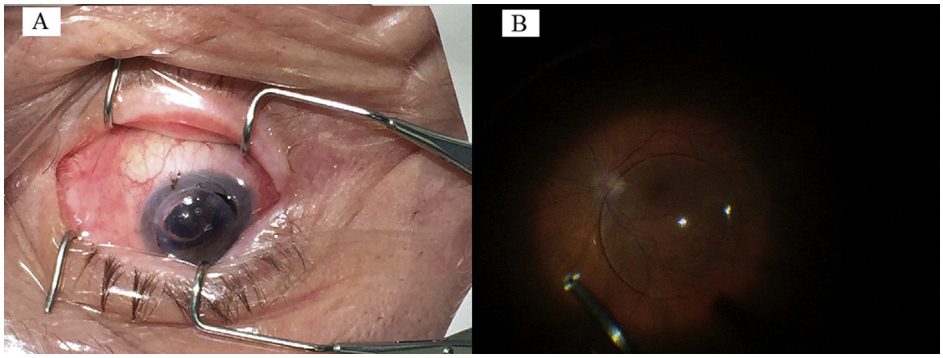

Rigid Gas Permeable Lens Intraocular Foreign Body following Blunt Trauma

A 76-year-old man with a history of penetrating keratoplasty (PK) for advanced keratoconus was struck in the eye by a fist, resulting in partial dehiscence of the graft and extrusion of the crystalline lens. Globe repair was performed with the existing graft (Fig 1**A**). Initial cornea clearing revealed the rigid gas permeable (RGP) lens the patient was wearing at the time of trauma, which was retained in the vitreous cavity with no sign of infection (Fig 1**B**). The graft eventually opacified and the patient underwent successful surgery with temporary keratoprosthesis, pars plana vitrectomy, removal of the RGP, and cornea graft placement (Magnified version of Fig 1A-B is available online at www.aaojournal.org).

Anton Vlasov, DO[1]
Eugene Milder, MD[2]
Paul Houghtaling, MD[1]

[1]Department of Ophthalmology, Walter Reed National Military Medical Center, Bethesda, Maryland; [2]Department of Ophthalmology, Fort Belvoir Community Hospital, Fort Belvoir, Virginia

Footnotes and Financial Disclosures

Disclaimer: The views expressed in this presentation are those of the author and do not reflect the official policy of the Department of Army/Navy/Air Force, Department of Defense or U.S. Government.